

1 **Activity-regulated growth of motoneurons at the neuromuscular  
2 junction is mediated by NADPH oxidases**

3 **Daniel Sobrido-Cameán<sup>1†</sup>, Matthew C. W. Oswald<sup>1, †</sup>, David M. D. Bailey<sup>1</sup> Amrita Mukherjee<sup>1</sup>  
4 and Matthias Landgraf<sup>1\*</sup>.**

5 <sup>1</sup>Department of Zoology, University of Cambridge, CB2 3EJ, Cambridge, UK

6 <sup>†</sup> contributed equally to this work

7

8 **\* Correspondence:**

9 Corresponding Author  
10 ml10006@cam.cam.uk

11

12 **Keywords:** motoneuron, plasticity, *Drosophila melanogaster*, reactive oxygen species, NADPH  
13 oxidase, Dual Oxidase, Nox, Aquaporin.

14

15 **Abstract**

16 Neurons respond to changes in the levels of activity they experience in a variety of ways,  
17 including structural changes at pre- and postsynaptic terminals. An essential plasticity signal required  
18 for such activity-regulated structural adjustments are reactive oxygen species (ROS). To identify  
19 sources of activity-regulated ROS required for structural plasticity *in vivo* we used the *Drosophila*  
20 larval neuromuscular junction as a highly tractable experimental model system. For adjustments of  
21 presynaptic motor terminals, we found a requirement for both NADPH oxidases, Nox and Dual  
22 Oxidase (Duox), that are encoded in the *Drosophila* genome. This contrasts with the postsynaptic  
23 dendrites from which Nox is excluded. NADPH oxidases generate ROS to the extracellular space.  
24 Here, we show that two aquaporins, Bib and Drip, are necessary ROS conduits in the presynaptic  
25 motoneuron for activity regulated, NADPH oxidase dependent changes in presynaptic motoneuron  
26 terminal growth. Our data further suggest that different aspects of neuronal activity-regulated structural  
27 changes might be regulated by different ROS sources: changes in bouton number require both NADPH  
28 oxidases, while activity-regulated changes in the number of active zones might be modulated by other  
29 sources of ROS. Overall, our results show NADPH oxidases as important enzymes for mediating  
30 activity-regulated plasticity adjustments in neurons.

31

32

### 33 1 Introduction

34        Reactive oxygen species (ROS) have commonly been associated with detrimental processes  
35 such as oxidative stress, toxicity, ageing, neurodegeneration and cell death because increases in ROS  
36 levels seen with ageing and neurodegenerative disorders, including Parkinson's (Spina and Cohen;  
37 1989) and Alzheimer's disease (Martins et al; 1986). However, it is appreciated that ROS are not  
38 simply cytotoxic agents, but more generally function as signalling molecules in a multitude of  
39 processes, including growth factor signalling (Suzukawa et al., 2000; Goldsmit et al., 2001; Kamata et  
40 al., 205; Nitte et al., 2010), wound healing (Razzell et al; 2013) and in development (Milton et al.,  
41 2011; Oswald et al; 2018a; Dhawan et al., 2020; for a reviews see Owusu-Ansah and Banerjee, 2009;  
42 Massaad and Klann, 2011; Wilson and Gonzalez-Billaut, 2015; Oswald et al., 2018b; Terzi and Suter,  
43 2020).

44        During nervous system development, ROS signalling is involved at all stages, from  
45 neurogenesis to pathfinding to synaptic transmission (Knapp and Klann, 2002; Kishida and Klann,  
46 2007; Massaad and Klann, 2011; Wilson and Gonzalez-Billaut, 2015; Wilson et al., 2018; Terzi and  
47 Suter, 2020). When studying ROS signalling *in vivo*, challenges include the ability to disentangle cell  
48 autonomous from indirect or systemic effects; or to determine sources and types of ROS. Using the  
49 fruit fly, *Drosophila melanogaster*, as a highly tractable experimental model system, genetic  
50 manipulations targeted to single motoneurons were able to identify hydrogen peroxide as a synaptic  
51 plasticity signal, generated as a consequence of neuronal overactivation and both necessary and  
52 sufficient for activity-regulated adaptive changes of synaptic terminal structure and transmission  
53 (Oswald et al., 2018; Dhawan et al., 2020). We found mitochondria to be a major source of activity-  
54 regulated hydrogen peroxide with opposing effects on the growth of pre- *vs* postsynaptic terminals: at  
55 the presynaptic terminal of the neuromuscular junction (NMJ) overactivation and hydrogen peroxide  
56 cause increases in terminals (Milton et al., 2011; Oswald et al., 2018). This change in presynaptic  
57 terminal growth is mediated by activation of the JNK signalling pathway (Milton et al., 2011), and it  
58 utilises the conserved Parkinson's disease-linked protein, DJ-1b, as a redox sensor, which regulates the  
59 PTEN-PI3 Kinase growth pathway (Oswald et al., 2018). In contrast, the size of postsynaptic dendritic  
60 arbors is negatively regulated by over-activation and activity-regulated hydrogen peroxide (Tripodi et  
61 al., 2008; Oswald et al., 2018; Dhawan et al., 2020). These studies using the *Drosophila* larval  
62 neuromuscular model system contrast with findings from cultured hippocampal neurons, which posit  
63 mitochondrially generated superoxide as the principal ROS signal downstream of over-activation  
64 (Hongpaisan et al. 2003; 2004). The extent to which both types of ROS operate as neuronal plasticity

65 signals downstream of over-activation remains to be resolved, though it is possible that apparent  
66 discrepancies might be due to the use of different cellular models and/or a reflection of the degree of  
67 overactivation.

68 Another principal source of ROS are NADPH oxidases, whose location in the plasma  
69 membrane could facilitate sub-cellular signalling discrete from mitochondrial ROS production.  
70 NADPH oxidases are integral membrane proteins that mediate a single electron transfer from NADPH  
71 to oxygen, thereby converting it to superoxide (Lambeth, 2002). These enzymes are prevalent  
72 throughout the evolutionary ladder from Amoebozoa and fungi to higher plants and mammals. NADPH  
73 oxidases are involved in growth and plasticity during nervous system development (Kishida et al.,  
74 2006; Munnamalai and Suter, 2009; Munnamalai et al., 2014; Olguín-Albuerne and Morán, 2015;  
75 Serrano et al., 2003; Tejada- Simon et al., 2005; Wilson et al., 2015; Wilson et al., 2016; Terzi and  
76 Suter, 2020). In contrast to mammalian genomes, which encode seven Nox isoforms (Nox 1-5, Duox  
77 1 and 2) (Lambeth et al., 2002; Kawahara et al., 2007), *Drosophila melanogaster* encodes just two  
78 NADPH oxidases: dual oxidase (*Duox*) and a Nox-5 homolog (*Nox*). Enzymatic activity of both is  
79 calcium-regulated, via their N-terminal calcium binding EF-hands (Razzell et al, 2013; Ha et al.,  
80 2005b, 2009; S. Moreira et al., 2010). Curiously, the mouse genome does not encode a calcium-  
81 regulated Nox-5 homologue, which has therefore not been studied extensively *in vivo* (Kawahara et al,  
82 2004). Recently, we identified the NADPH oxidase Duox as necessary in motoneurons to reduce their  
83 dendritic arbors in response to neuronal over-activation, an adaptive response to reduce the numbers  
84 of presynaptic inputs and thus synaptic drive (Zwart et al., 2013; Dhawan et al., 2020). We further  
85 found that these activity-regulated ROS generated by Duox at the extracellular face of the plasma  
86 membrane, required the aquaporins, Bib and Drip; presumably for efficient entry into the cytoplasm to  
87 regulate dendritic growth and/or stability (Dhawan et al., 2020).

88 Here, we investigated the role of NADPH oxidases at the presynaptic terminal of the NMJ,  
89 whose growth response to neuronal over-activation is distinct to that of the dendritic compartment of  
90 the motoneuron. We show that the NADPH oxidases Duox and Nox are sources of activity-regulated  
91 ROS that mediate activity-regulated growth of NMJ terminals. In contrast to motoneuron dendrites,  
92 both NADPH oxidases function at the presynaptic NMJ, necessary and sufficient to elicit changes in  
93 growth. At the NMJ too, we find the aquaporins, Bib and Drip, are necessary for autocrine signalling  
94 at the NMJ. This arrangement at the presynaptic NMJ terminal contrasts with their dendritic function  
95 within these motoneurons, where only Duox, but not Nox, is required. This differential requirement of  
96 Nox mirrors its sub-cellular localisation, with Nox largely excluded from dendrites. Furthermore, at

97 the postsynaptic compartment extracellular ROS, including from other neurons in the vicinity, act as  
98 local plasticity signals that cause reductions in dendritic arbor size (Dhawan et al., 2020).

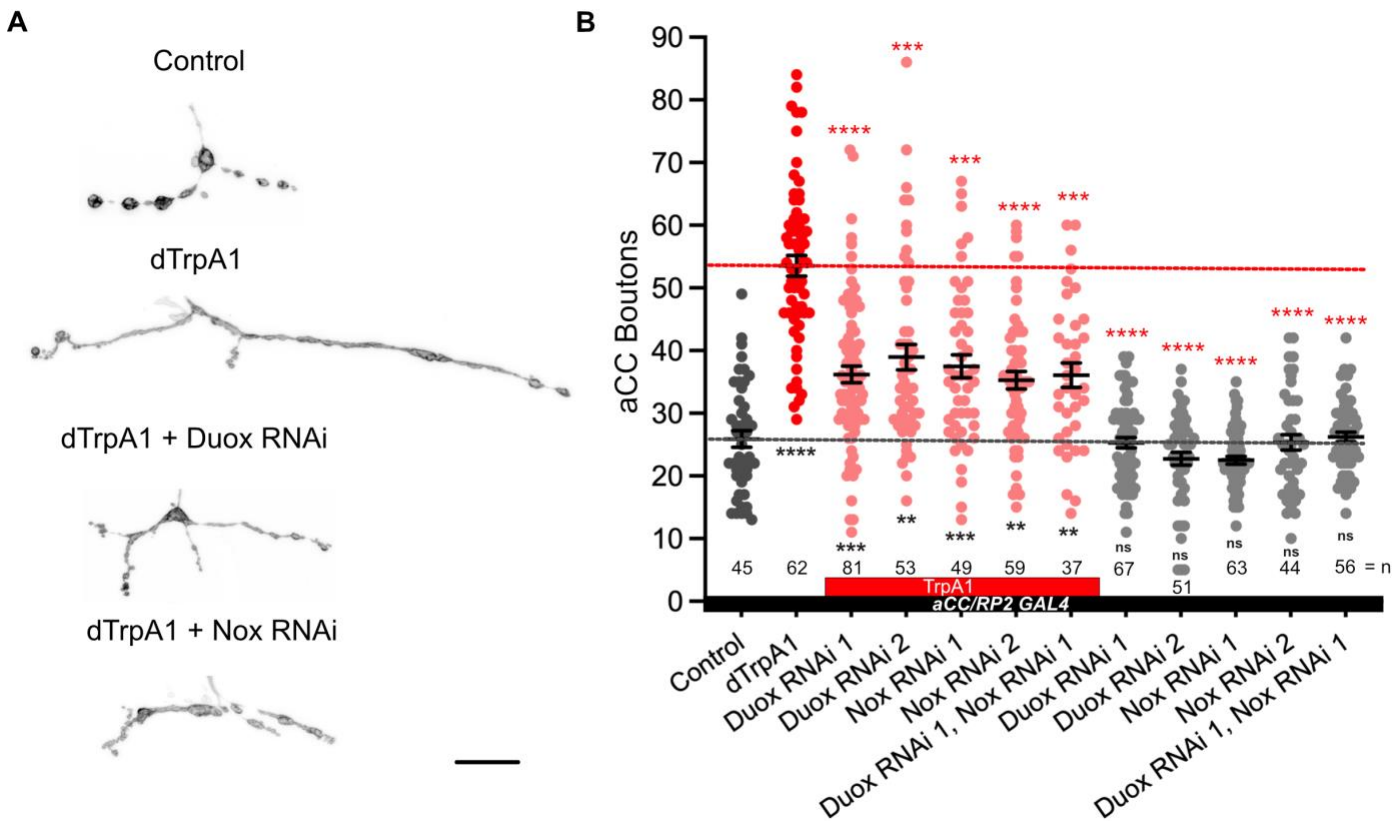
99

100 **2 Results**

101 **NADPH oxidases, Duox and Nox, are both required for activity-regulated growth at the**  
102 **neuromuscular junction.**

103 Mitochondria are a major source of activity-generated ROS, notably within the cytoplasm. Here,  
104 we sought to investigate the role of membrane localised ROS generators, the NADPH oxidases Nox  
105 and Duox, during activity-regulated adjustment of presynaptic terminals. As a highly tractable  
106 experimental model we used the well characterised neuromuscular junction (NMJ) of the *Drosophila*  
107 larva (Frank et al., 2013). Specifically, we focused on the NMJ of the so called ‘anterior Corner Cell’  
108 (aCC), which innervates the most dorsal body wall muscle, known as muscle 1 (Crossley 1978) or  
109 dorsal acute muscle 1 (DA1) (Sink and Whitington, 1991; Landgraf et al., 1997; Baines et al., 1999;  
110 Baines et al., 2001; Bate, 1993; Choi et al., 2004; Hoang and Chiba, 2001). For cell-specific over-  
111 activation of aCC motoneurons, we used the established paradigm of targeted mis-expression of the  
112 warmth-gated cation channel, dTRPA1 (Hamada et al., 2008; Oswald et al., 2018; Dhawan et al.,  
113 2020). This allows aCC motoneurons to be selectively over-activated simply by placing larvae at  
114 >24°C, the temperature threshold for dTRPA1 ion channel opening (Pulver et al., 2009).

115 First, we re-confirmed that at 25°C *dTrpA1* expression in aCC motoneurons leads to significant  
116 increases in bouton number at the aCC-DA1 NMJ relative to non-manipulated controls, as previously  
117 shown (Oswald et al., 2018) (Figure 1). An advantage of using cell-specific dTRPA1-mediated activity  
118 manipulations in this system is that these can be carried out at 25°C, a temperature considered optimal  
119 for *Drosophila melanogaster* development (Lachaise et al., 1988; Pool et al., 2012) and therefore  
120 generally considered neutral, while sufficient to mildly activate neurons that mis-express dTRPA1  
121 (Pulver et al., 2009; Tsai et al., 2012).



122

123 **Figure 1. NADPH oxidases, dDuox and dNox, are both required for activity-regulated growth**  
124 **of the neuromuscular junction.** A) Representative images of aCC motoneuron terminals on their  
125 target muscle, DA1 [muscle 1, according to (Crossley, 1978)] in third instar larvae (100 hr ALH):  
126 control; dTrpA1 overactivated; dTrpA1 overactivated while either Duox or Nox is concomitantly  
127 knocked down via targeted RNAi (“TrpA1 + Duox KD” and “TrpA1 + Nox KD”). B) Dot-plot  
128 quantification shows NMJ bouton number increases in response to cell-specific activity increases.  
129 This phenotype is rescued by simultaneous NADPH oxidase knockdown. Triangles represent  
130 presence of UAS-dTrpA1 activity manipulation, while circle indicate absence of dTrpA1.  
131 Mean  $\pm$  SEM, ANOVA, \*\*  $p < 0.01$ , \*\*\*  $p < 0.001$ , \*\*\*\*  $p < 0.0001$ . Red asterisks indicate  
132 comparisons with the UAS-TrpA1 over-activation group, while black indicate comparison with the  
133 un-manipulated wild type control. Scale bar = 20  $\mu$ m.

134

135

136

137

138 Next, we tested the requirement for the two NADPH oxidases encoded in the *Drosophila* genome,  
139 *Duox* and *Nox*, in mediating these activity-regulated structural changes at the NMJ. To this end, we  
140 expressed RNAi transgenes for knocking down endogenous *Duox* or *Nox* in aCC motoneurons. By  
141 themselves, expression of *UAS-Duox-RNAi* or *UAS-Nox-RNAi* transgenes in aCC motoneurons have  
142 no measurable effect on NMJ morphology. However, in motoneurons that have been overactivated by  
143 *UAS-dTrpA1*, the characteristic activity-induced bouton overgrowth phenotype is suppressed by co-  
144 expression of *UAS-Duox-RNAi* or *UAS-Nox-RNAi* transgenes, individually or combined (Figure 1).  
145 Neuronal overactivation by *UAS-dTrpA1* also causes a reduction in active zone numbers (Oswald et  
146 al., 2018). We find no statistically significant changes in active zone number following NADPH  
147 oxidases manipulations (Supplementary figure 1). These results show that the membrane localised  
148 ROS generators, *Nox* and *Duox*, are required primarily for activity-regulated changes in presynaptic  
149 terminal growth while not significantly impacting on the number of presynaptic release sites.

150

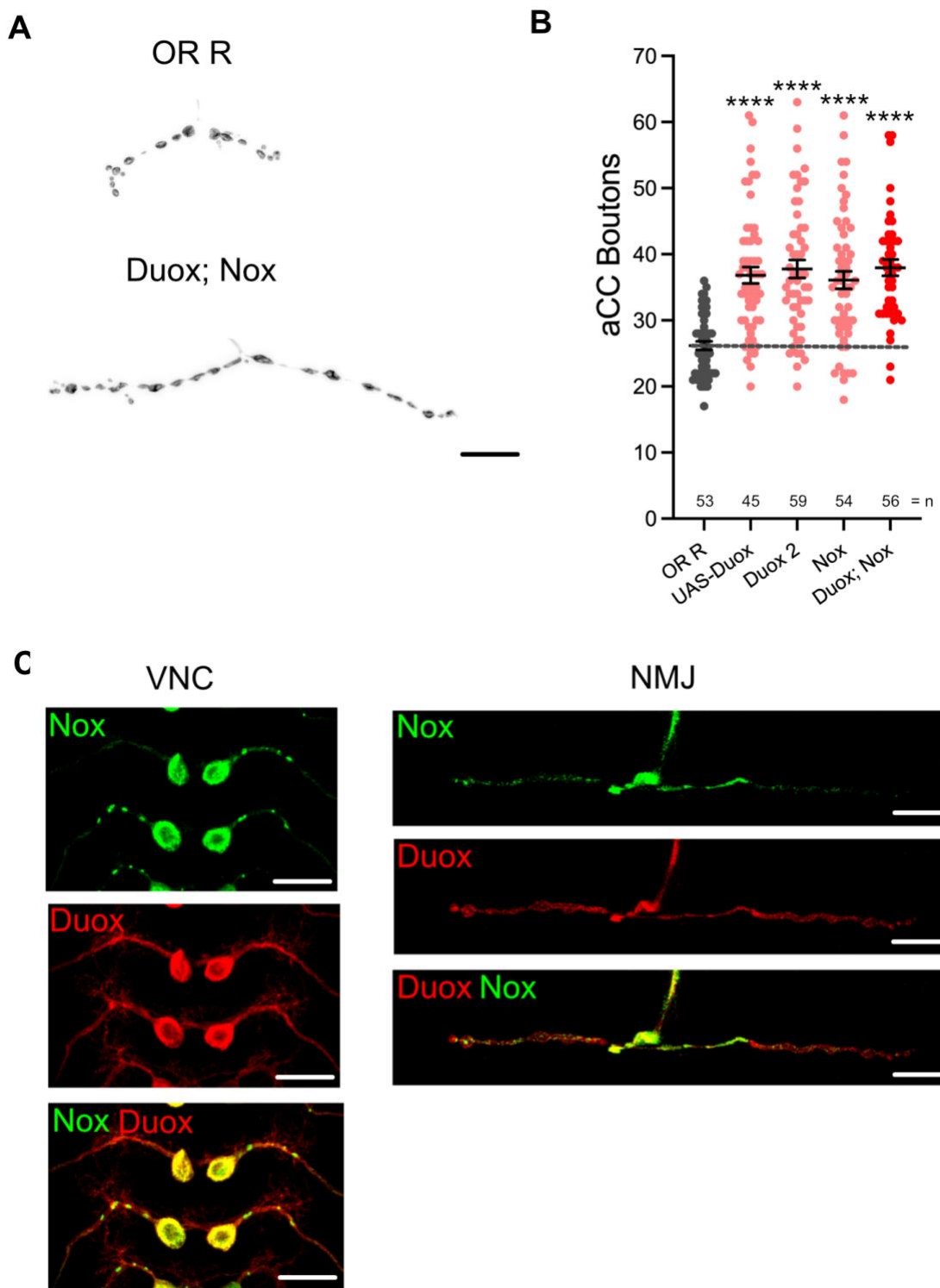
151

## 152 **Duox and Nox activity is sufficient for mediating structural changes at the NMJ**

153 We next asked if the activity of these NADPH oxidases might also be sufficient for regulating  
154 presynaptic terminal growth. To test this, we overexpressed *UAS-Duox* or *UAS-Nox* transgenes in aCC  
155 motoneurons. Quantification showed comparable increases in bouton number at the NMJ as a  
156 consequence of over-expression of either *Duox* or *Nox*. No enhancement of this phenotype occurs  
157 when both are co-expressed (Figure 2). In contrast, active zone numbers are not significantly impacted  
158 by overexpression of either NADPH oxidase (Supplementary figure 1).

159 For the postsynaptic compartment, namely the dendritic arbor of motoneurons, we had previously  
160 shown that only *Duox*, but not *Nox*, has a role in activity-regulated plasticity (Dhawan et al., 2020).  
161 To further explore this difference in NADPH oxidase requirement between pre- vs postsynaptic  
162 compartments, we generated tagged transgenes of both NADPH oxidases, *UAS-Duox::mRuby2::HA*  
163 and *UAS-Nox::YPet*. When expressed in aCC motoneurons to reveal sub-cellular localisation, we see  
164 exclusion of *Nox::YPet* from the postsynaptic dendrites, while *Duox::mRuby2::HA* is fairly  
165 homogeneously distributed within the plasma membrane (Figure 2C). These patterns of distinct sub-  
166 cellular distributions, notably exclusion of *Nox::YPet* from dendrites, are compatible with the genetic  
167 manipulations phenotypes and point to *Nox* being selectively sorted to soma and presynaptic  
168 compartments in these neurons.

169



170

171 **Figure 2. dDuox or dNox activity is sufficient for mediating structural changes at the NMJ.** A)  
172 Representative images of aCC presynaptic terminals on muscle DA1 from third instar larvae (100  
173 hr ALH) of control aCC and those overexpressing Duox and Nox. B) Dot-plot quantification shows  
174 NMJ bouton number increases in response to cell-specific over-expression of NADPH oxidases. C)

175 *Duox and Nox, localization in neurons: representative confocal micrograph images of aCC somata*  
176 *and dendrites in the ventral nerve cord (VNC) and aCC presynaptic terminals at the DA1 muscle*  
177 *in third instar larvae (72 hr ALH), showing subcellular localisation of tagged over-expressed*  
178 *Duox::mRuby2::HA (in red) and Nox::YPet (in green). Mean  $\pm$  SEM, ANOVA, \*\*\*\* p<0.0001.*  
179 *Comparisons are made with the control group. Scale bar = 20  $\mu$ m.*

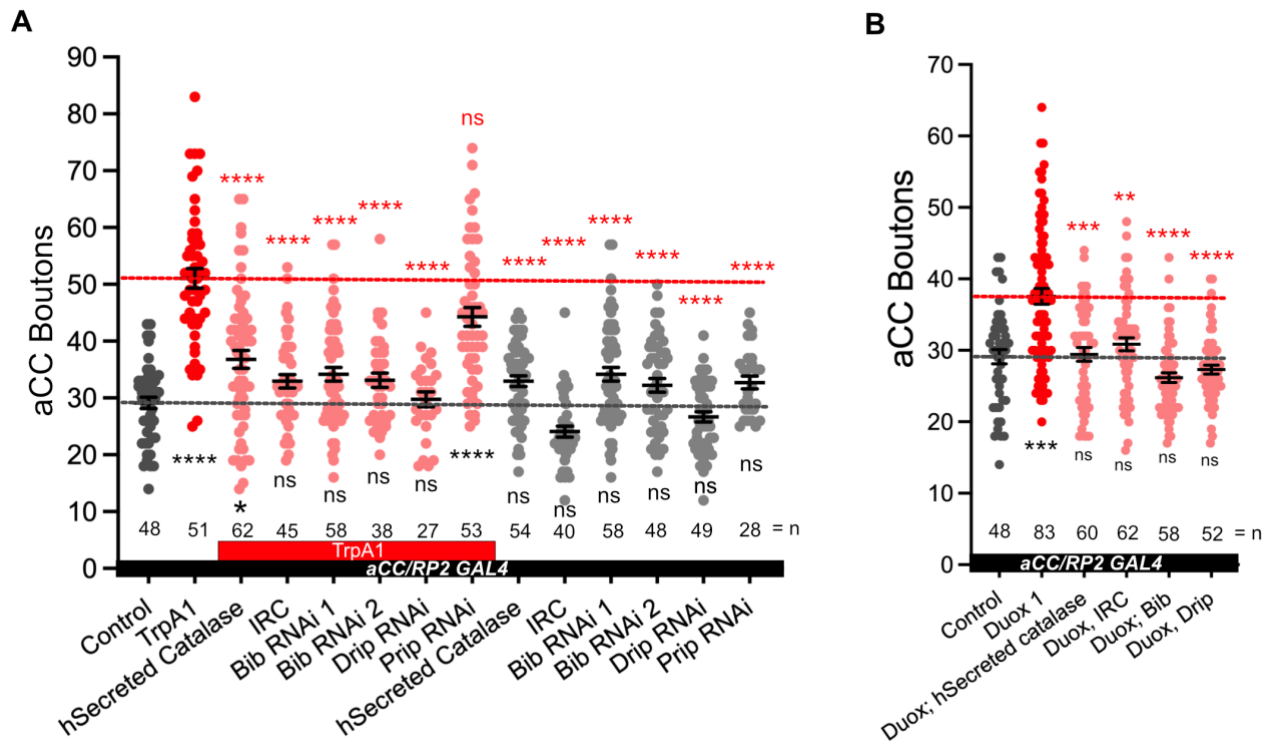
180  
181  
182

183 **Aquaporin channel proteins Bib and Drip are necessary for NADPH oxidase-regulated**  
184 **structural changes at the NMJ**

185 The NADPH oxidases Duox and Nox are transmembrane proteins that generate ROS at the  
186 extracellular face of the plasma membrane (Lambeth, 2002; Panday et al., 2015). We reasoned that if  
187 NADPH oxidase-generated ROS are indeed instrumental in activity-regulated adjustment of synaptic  
188 terminals, then neutralisation of extracellular ROS should rescue NMJ phenotypes associated with  
189 NADPH oxidase overexpression. To test this, we mis-expressed in aCC motoneurons two different  
190 forms of catalases that are secreted to the extracellular space; a human version and the *Drosophila*  
191 immune-regulated catalase (Irc) (Ha et al., 2005b; Fogarty et al., 2016). These catalases neutralise  
192 extracellular hydrogen peroxide by conversion to water. On their own, their mis-expression in aCC  
193 motoneurons has no significant impact on NMJ structure or size. To test the model of neuronal activity  
194 leading to NADPH oxidase activation, leading to extracellular ROS production, we co-expressed  
195 secreted catalase in aCC motoneurons while over-activating these with dTRPA1. The presence of a  
196 secreted catalase suppresses the NMJ growth that would otherwise ensue with neuronal overactivation  
197 (Figure 3A). Similarly, NMJ over-growth stimulated by over-expression of Duox is also neutralised  
198 by co-expression of secreted catalase in the same neuron (Figure 3B). These experiments demonstrate  
199 that it is the presence of extracellular ROS, notably hydrogen peroxide generated by NADPH oxidases,  
200 which leads to activity-induced changes in NMJ growth.

201 Because NAPDH oxidases generate ROS extracellularly, we wanted to explore how extra-cellular  
202 ROS might enter the cell so as to act on intracellular signalling pathways that would regulate NMJ  
203 growth. Several studies, including one from this lab, have postulated a role for aquaporin channels,  
204 specifically those encoded by the genes *bib* and *Drip* (Albertini and Bianche, 2010; Dhawan et al.,  
205 2020; Dutta and Das, 2022). Indeed, for the presynaptic NMJ, we found that co-expression of *UAS-*  
206 *RNAi* constructs designed to knock down *bib* or *Drip*, but not those for *prip*, rescue NMJ growth  
207 phenotypes caused by dTRPA1-mediated overactivation. Expression of the *UAS-RNAi* constructs alone

208 had no significant effect (Figure 3A). To further test the model that extracellular ROS generated by  
 209 NADH oxidases cause structural change at the NMJ, we overexpressed Duox in aCC motoneurons and  
 210 at the same time co-expressed *UAS-RNAi* constructs designed to knock down the aquaporin channel  
 211 proteins Bib or Drip. In those neurons the Duox gain-of-function NMJ growth phenotype is fully  
 212 rescued (Figure 3B).



213

214

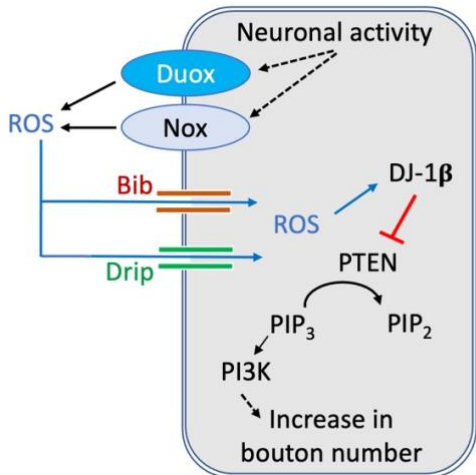
215 **Figure 3. Aquaporins Bib and Drip are required for activity-regulated plasticity at the**  
 216 **neuromuscular junction.** A) Dot-plot quantification shows NMJ bouton number increases in  
 217 response to cell-specific activity and the rescue of the phenotype when secreted catalases are  
 218 expressed or aquaporins Bib or Drip are knock down. When the RNAi lines are represented by  
 219 triangles, it indicates that it is in combination with dTrpA1, when the RNAi lines are represented  
 220 by circles, it is without dTrpA1. B) Dot-plot quantification shows NMJ bouton number increases in  
 221 response Duox and the rescue of the phenotype when secreted catalases are expressed or  
 222 aquaporins Bib or Drip are knock down. Mean  $\pm$  SEM, Kruskal-Wallis test, \* $p < 0.05$ , \*\* $p < 0.01$ ,  
 223 \*\*\* $p < 0.001$ , \*\*\*\* $p < 0.0001$ . Comparisons are made with the TrpA1 group in A and with Duox  
 224 group in B.

225

226

227 In summary, our observations suggest that at the presynaptic NMJ, neuronal overactivation leads  
228 to activation of both NADPH oxidases, Duox and Nox, at the plasma membrane. These enzymes  
229 generate ROS at the extracellular face, which are then brought into the cytoplasm by aquaporin  
230 channels comprising Bib and Drip. Inside the cell, the ROS act on intracellular membrane-localised  
231 signalling pathways that regulate synaptic terminal structure and size, including the phosphatase PTEN  
232 and DJ-1 $\beta$ , as previously shown (Figure 4) (Oswald et al., 2018).

233



234

235

236 **Figure 4. Model of activity-regulated plasticity at the neuromuscular junction mediated by ROS**  
237 **signalling.** Neuronal activity leads to activation of both calcium regulated NADPH oxidases, Duox  
238 and Nox, at the presynaptic motoneuron terminal. Extracellularly generated ROS reintroduced into  
239 the presynaptic cytoplasm via aquaporin channels, including Bib and Drip. ROS modulated  
240 PI3Kinase signalling at the plasma membrane via oxidation of DJ-1 $\beta$ , which when oxidised  
241 increases binding and inhibition of the PTEN phosphatase, thus causing increased PI3Kinase  
242 signalling activity, stimulating growth and addition of synaptic release sites.

243

244

### 245 3 Discussion

246

247 ROS have increasingly been recognised as signalling molecules required for nervous system  
248 development and function, from regulating the dynamics of the growth cone cytoskeleton to synaptic  
249 transmission and learning (see Terzi and Suter, 2020). At the Drosophila NMJ, ROS have been shown

250 necessary for activity-induced synaptic terminal growth (Oswald et al., 2018). ROS have also been  
251 shown causative and sufficient to induce changes at synaptic terminals; when accumulating as a result  
252 of physiological dysfunction, leading to oxidative stress (Milton et al., 2011), or following  
253 manipulations that increase ROS levels (Milton et al., 2011; Hussain et al., 2018; Peng et al. 2019).  
254 While mitochondria are a major source of cellular ROS (Murphy, 2009; Zorov et al., 2014; Sanz, 2016),  
255 it has remained unclear to what extent mitochondrial ROS directly impact on events at the plasma  
256 membrane, such as modulation of PTEN-PI3Kinase signalling, which regulates synaptic terminal  
257 growth (Acebes, et al., 2012; Jordán-Álvarez et al., 2012; Martín-Peña et al., 2006; Oswald et al, 2018),  
258 or oxidation of ion channel subunits that modulate neuronal excitability (Kempf et al., 2019).  
259

## 260 **Differential requirements for NADPH oxidases in pre- vs postsynaptic compartments**

261 In this study we focused on NADPH oxidases as generators of ROS that are ideally positioned to  
262 influence signalling at the plasma membrane. Working with the NMJ in the *Drosophila* larva as an  
263 experimental *in vivo* model system, we demonstrated that both NADPH oxidases, Nox and Duox, are  
264 required for activity-induced growth (Figure 1). Both enzymes are endowed with N-terminal calcium  
265 binding EF-hand motifs, linking their activity to intracellular calcium levels, as shown for *Drosophila*  
266 Duox (Ha et al; 2009; Rigo et al., 2009; Razzell et al., 2013) and the vertebrate homologue, Nox5  
267 (Bánfi et al., 2004; Millana et al., 2020). Conversely, over-expression of either enzyme is sufficient to  
268 phenocopy such presynaptic terminal growth (Figure 2). Curiously, the requirement for NADPH  
269 oxidases in regulating dendritic growth is different, with only Duox, but not Nox, mediating activity-  
270 induced reduction of dendritic arbor size (Dhawan et al., 2020). This difference in pre- *versus*  
271 postsynaptic compartment regulation is mirrored by their differential sub-cellular localisation, with  
272 tagged Nox protein being effectively excluded from the postsynaptic dendritic arbors, unlike Duox  
273 (Figure 2C). Apart from this differential requirement in pre- *versus* postsynaptic compartments, it is  
274 unclear to what extent Nox and Duox might perform different functions during activity-induced  
275 growth. At the NMJ, where both are present and required, we found no difference in phenotypes  
276 following RNAi knockdown or mis-expression. Curiously, phenotypes were also comparable  
277 regardless of whether the expression of both enzymes was manipulated simultaneously or individually,  
278 suggesting either a saturation of phenotype or, speculatively, that Nox and Duox might operate in the  
279 same signalling pathway with their activation contingent on one another.

280  
281  
282

## 283 NADPH oxidases generate extracellular ROS and mediate autocrine signalling

284 Because Nox and Duox generate ROS at the extracellular face they have the potential for inter-  
285 cellular signalling, for example as documented during wound healing (Razzell et al, 2013; Niethammer  
286 et al., 2009, 2016). Indeed, within the dense meshwork of neuronal processes and synapses of the CNS,  
287 we recently found that reduction of extracellular hydrogen peroxide in the immediate vicinity of  
288 dendritic processes (by mis-expression of a secreted catalase) or attenuation of ROS entry into those  
289 dendrites (by knock-down of aquaporins), both cause significant dendritic over-growth (Dhawan et al.,  
290 2020). This suggests that within the densely innervated central neuropile, extracellular ROS generated,  
291 including those from activity-regulated NADPH oxidases, might function as local signals to which  
292 neurons respond with adjustments of their synaptic terminals. This contrasts with the peripheral  
293 Drosophila larval NMJ, where we did not see any significant changes in synaptic terminal morphology  
294 following manipulations that would either reduce entry of ROS into the presynaptic terminal or  
295 reductions of extracellular ROS (Figure 3). These observations suggest that at the presynaptic NMJ,  
296 NADPH oxidases might be required only under conditions of elevated neuronal activity. While these  
297 data further suggest that at the presynaptic NMJ, NADPH oxidase-generated ROS are principally  
298 engaged in autocrine signalling, we cannot currently exclude the potential for inter-cellular signalling  
299 to adjacent muscles and glia.

300 Autocrine ROS signalling at both pre- and postsynaptic compartments is underlined by the  
301 requirement for the aquaporin channel proteins, Bib and Drip (Figure 3) (Dhawan et al., 2020). Some  
302 studies have questioned the extent to which Bib might function as an aquaporin, as unable to form  
303 effective water channels in a heterologous expression system (Tatsumi et al., 2009; Kourghi et al.,  
304 2017). However, in this and in a previous study (Dhawan et al., 2020), Bib RNAi knockdown produces  
305 synaptic terminal phenotypes indistinguishable from knockdown of Drip, or from mis-expression of  
306 secreted forms of catalase (Dhawan et al., 2020). This suggests that Bib functions in the same pathway  
307 as the aquaporin Drip, potentially forming part of a heteromeric channel with permeability for  
308 hydrogen peroxide.

309

## 310 Independent, local regulation of pre- and postsynaptic terminal growth

311 Over-activation of neurons results in changes to both pre- and postsynaptic terminals, though it has  
312 been unclear in how far such changes in growth of input and output compartments might be co-  
313 ordinatorily regulated. Working with this experimental system we happen to have identified two sets of  
314 manipulations that suggest the growth of pre- and postsynaptic terminals can be regulated  
315 independently of each other. First, in motoneurons that have been over-activated by mis-expression of

316 dTRPA1, RNAi knockdown of Nox has no effect on the activity-induced reduction of the postsynaptic  
317 dendrites, which receive all synaptic input from pre-motor interneurons (as Nox protein appears to be  
318 excluded from dendrites); yet at the output compartment, the presynaptic NMJ, of those same neurons,  
319 activity-linked overgrowth is significantly suppressed by knockdown of Nox. This contrasts with the  
320 effect of Duox knockdown under conditions of neuronal over-activation, with Duox RNAi suppressing  
321 over-activation phenotypes effectively at both pre- and postsynaptic terminals.

322 Second, RNAi knockdown alone of the genes coding for aquaporin channel proteins Bib or Drip  
323 cause significant dendritic overgrowth, without affecting the presynaptic NMJ. These manipulations  
324 suggest that, at least in Drosophila larval motoneurons, synaptic terminal growth can be regulated  
325 locally through ROS signalling, such that pre- and postsynaptic compartments can adjust independently  
326 from each other. This makes sense when viewing extracellular ROS as local signals for over-activation,  
327 to which cells respond by adjusting their synaptic terminals. In this context, it remains to be seen to  
328 what extent extracellular ROS might impact on the regulation of synaptic transmission.

329 In summary, it is increasingly appreciated that ROS are important signals, whose signalling  
330 capability is proportional to the spatiotemporal precision attained. Sub-cellular specificity of ROS  
331 generators, such as the NAPDH oxidases studied here, is an important facet.

332  
333  
334  
335  
336

337 **4 Materials and Methods**

338 **Fly genetics**

339 *Drosophila melanogaster* strains were maintained on a standard apple juice-based agar medium at  
340 25°C. The following fly strains were used: *OregonR* (#2376 Bloomington Drosophila Stock  
341 Center), *UAS-dTrpA1* in attP16 (Hamada et al., 2008; FBtp0089791), *UAS-Duox.RNAi* (1) (#32903  
342 BDSC; FBtp0064955), *UAS-Duox.RNAi* (2) (#38916 BDSC; FBgn0283531), *UAS-Nox.RNAi* (1) (Ha  
343 et al., 2005b; FBal0191562), *UAS-Nox.RNAi* (2) (#32433 BDSC; FBgn0085428), *UAS-bib.RNAi* (1)  
344 (#57493 BDSC; FBtp0096443), *UAS-bib.RNAi* (2) (#27691 BDSC; FBtp0052515), *UAS-*  
345 *Drip.RNAi* (1) (#44661 BDSC; FBtp0090566), *UAS-Drip.RNAi* (2) (#106911  
346 Vienna Drosophila Resource Centre; FBtp0045814) (Begland et al., 2012), *UAS-Prip.RNAi* (2)  
347 (#44464 BDSC; FBtp0090258), *UAS-Duox* (1) (Ha et al., 2005b), *UAS-Duox::mRuby2::HA* (2) (this

348 paper), *UAS-Nox::YPet* (this paper), *UAS-hCatS* (*human secreted catalase*) (FBal0190351; Ha et al.,  
349 2005b; Fogarty et al., 2016), *UAS-extracellular immune-regulated catalase* (*Irc*) (FBal0191070, Ha et  
350 al., 2005b).

351 Transgene expression was carried out at 25°C, unless otherwise noted, targeted to RP2 and aCC  
352 motoneurons using the following Gal4 expression line: *RN2-O-Gal4*, *UAS-FLP*, *tubulin84b-FRT-CD2-FRT-Gal4*; *RRFa-Gal4*, *20xUAS-6XmCherry::HA* (Pignoni and Zipursky, 1997; Fujioka et al.,  
353 2003; Shearin et al., 20014). Briefly, RN2-GAL4 expression in RP2 and aCC motoneurons is restricted  
354 to the embryo, but is maintained subsequently by FLPase-gated *tubulin84B-FRT-CD2-FRT-GAL4* (Ou et al., 2008). mCherry::HA was used as morphological reporter. To study the localisation  
355 of the tagged *Nox::YPet* and *Duox::mRuby2::HA* transgene expression was targeted to aCC  
356 motoneurons using the *GMR94G06-Gal4* (#40701 BDSC; FBgn0053512; Pérez-Moreno and O'Kane,  
357 2019). *pJFRC12-10XUAS-IVS-Nox-YPet* (GenBank OP716753) in landing site VK00040 [cytogenetic  
358 location 87B10] was generated by Klenow assembly cloning ([tinyurl.com/4r99uv8m](http://tinyurl.com/4r99uv8m)). Briefly, from  
359 *pJFRC12-10XUAS-IVS-myr-GFP* plasmid DNA we removed the coding sequence for *myr::GFP*  
360 using *Xho*I and *Xba*I, and replaced it with *Nox* cDNA from DGRC clone FI15205 (*pOTB7* vector  
361 backbone; kindly provided by Kenneth H. Wan, DGRC Stock 1661239 ;  
362 <https://dgrc.bio.indiana.edu/stock/1661239> ; RRID:DGRC\_1661239), its 3' stop codon replaced by a  
363 flexible glycine-serine linker, followed by YPet (Nguyen and Daugherty, 2005). Similarly, we created  
364 *pJFRC12-10XUAS-IVS-Duox-mRuby2-HA* (GenBank OP716753) in landing site VK00022  
365 [cytogenetic position 57A5] using *Duox* cDNA kindly provided by Won-Jae Lee, its 3' stop codon  
366 replaced by a flexible glycine-serine linker, followed by mRuby2 (Lam et al, 2012), followed by  
367 another glycine-serine flexible linker and four tandem repeats of the hemagglutinin (HA) epitope.  
368 Transgenics were generated via phiC31 integrase-mediated recombination (Bischof et al.; 2007) into  
369 defined landing sites by the FlyORF Injection Service (Zürich, Switzerland).  
370  
371

### 373 Dissections and immunocytochemistry

374 Flies were allowed to lay eggs on apple-juice agar based medium overnight at 25 °C. Larvae were then  
375 reared at 25°C on yeast paste, while avoiding over-crowding. Precise staging of the late wandering  
376 third instar stage was achieved by: a) checking that a proportion of animals from the same time-  
377 restricted egg lay had initiated pupariation; b) larvae had reached a certain size and c) showed gut-  
378 clearance of food (yeast paste supplemented with Bromophenol Blue Sodium Salt (Sigma-Aldrich)).  
379 Larvae were dissected in Sorensen's saline, fixed for 5 min at room temperature in Bouins fixative or

380 10 min paraformaldehyde (Agar Scientific) when staining for GFP/YPet epitopes, as previously  
381 detailed (Oswald et al., 2018). Wash solution was Sorensen's saline containing 0.3% Triton X-100  
382 (Sigma-Aldrich) and 0.25% BSA (Sigma-Aldrich). Primary antibodies, incubated overnight at 10°C,  
383 were: Goat-anti-HRP Alexa Fluor 488 (1:1000) (Jackson ImmunoResearch Cat. No. 123-545-021),  
384 Rabbit-anti-dsRed (1:1000) (ClonTech Cat. No. 632496), Mouse nc82 (Bruchpilot; Developmental  
385 Studies Hybridoma Bank Cat No nc82), Chicken anti-GFP (1:5000) (abcam Cat No ab13970);  
386 secondary antibodies, 2 hr at room temperature: Donkey anti-mouse Alexa Fluor 647; Donkey-anti-  
387 Rabbit CF568 (1:1200) (Biotium Cat. No. 20098), Donkey anti-Chicken CF488 (1:1000) (Cambridge  
388 Bioscience Cat No 20166) and goat anti-Rabbit Atto594 (1:1000) (Sigma-Aldrich Cat No 77671-1ML-  
389 F). Specimens were cleared in 70% glycerol, overnight at 4°C, then mounted in Mowiol.

390 **Image acquisition and analysis**

391 Specimens were imaged using a Leica SP5 point-scanning confocal, and a 63x/1.3 N.A. (Leica)  
392 glycerol immersion objective lens and LAS AF (Leica Application Suite Advanced Fluorescence)  
393 software. Confocal images were processed using ImageJ (to quantify active zones) and Affinity Photo  
394 (Adobe; to prepare figures). Bouton number of the NMJ on muscle DA1 from segments A3-A5 was  
395 determined by counting every distinct spherical varicosity along the NMJ branch.

396 To study if genetic manipulations targeted to aCC and RP2 motoneurons change muscle size  
397 we measured surface area of DA1 muscles, imaged under DIC optics using a Zeiss Axiophot compound  
398 microscope and a Zeiss Plan-Neofluar 10x/0.3 N.A. objective lens. Images were taken with an Orca  
399 CCD camera (Hamamatsu) and muscle surface area was determined using ImageJ by multiplying  
400 muscle length by width. Quantification of key representative experiments, covering most transgenic  
401 lines used and conditions where genetic manipulation of aCC motoneurons cause significant changes  
402 in bouton number, show no statistically significant differences in average muscle size, which is used  
403 as an indicator of overall animal size. Correlation between individual muscle sizes and bouton numbers  
404 show that the biggest differences in muscle surface area is due to dissection artefact of differences to  
405 the extent that larval filets are stretched, rather than differences in animal or muscle growth, which  
406 would lead to clear correlations between measured muscle surface area and NMJ bouton number (see  
407 supplementary figure 2). Taking account of this, bouton numbers are shown as raw counts, not  
408 normalized to average muscle surface area.

409

410

411        Representative schematics, drawings and plates of photomicrographs were generated with  
412 Affinity Photo (Serif Ltd., United Kingdom).

413        **Statistical analysis**

414        All data handling was performed using Prism software (GraphPad). NMJ bouton number data  
415 was tested for normal/Gaussian distribution using the D'Agostino-Pearson omnibus normality test.  
416 When normal distribution was confirmed the statistically comparisons were done using one-way  
417 analysis of variance (ANOVA), with Tukey's multiple comparisons test. When non-normal  
418 distribution was confirmed the statistically comparisons were done using Kruskal-Wallis test.

419

420

421

422        **5 References**

423        Acebes, A., & Morales, M. (2012). At a PI3K crossroads: lessons from flies and  
424 rodents. *Reviews in the neurosciences*, 23(1), 29–37. <https://doi.org/10.1515/rns.2011.057>

425        Albertini, R., & Bianchi, R. (2010). Aquaporins and glia. *Current neuropharmacology*, 8(2),  
426 84–91. <https://doi.org/10.2174/157015910791233178>

427        Baines, R. A., Robinson, S. G., Fujioka, M., Jaynes, J. B., & Bate, M. (1999). Postsynaptic  
428 expression of tetanus toxin light chain blocks synaptogenesis in *Drosophila*. *Current biology*:  
429 CB, 9(21), 1267–1270. [https://doi.org/10.1016/s0960-9822\(99\)80510-7](https://doi.org/10.1016/s0960-9822(99)80510-7)

430        Baines, R. A., Uhler, J. P., Thompson, A., Sweeney, S. T., & Bate, M. (2001). Altered electrical  
431 properties in *Drosophila* neurons developing without synaptic transmission. *The Journal of  
432 neuroscience: the official journal of the Society for Neuroscience*, 21(5), 1523–1531.  
433 <https://doi.org/10.1523/JNEUROSCI.21-05-01523.2001>

434        Bánfi, B., Tirone, F., Durussel, I., Knisz, J., Moskwa, P., Molnár, G. Z., Krause, K. H., & Cox,  
435 J. A. (2004). Mechanism of Ca<sup>2+</sup> activation of the NADPH oxidase 5 (NOX5). *The Journal of  
436 biological chemistry*, 279(18), 18583–18591. <https://doi.org/10.1074/jbc.M310268200>

437        Bánfi, B., Tirone, F., Durussel, I., Knisz, J., Moskwa, P., Molnár, G. Z., Krause, K. H., & Cox,  
438 J. A. (2004). Mechanism of Ca<sup>2+</sup> activation of the NADPH oxidase 5 (NOX5). *The Journal of  
439 biological chemistry*, 279(18), 18583–18591. <https://doi.org/10.1074/jbc.M310268200>

440 Bate M. 1993. The mesoderm and its derivatives. In: Bate C. M., Martinez-Arias A (Eds). The  
441 Development of *Drosophila Melanogaster*. Cold Spring Harbor: The development of *Drosophila*  
442 *melanogaster*.

443 Bergland, A. O., Chae, H. S., Kim, Y. J., & Tatar, M. (2012). Fine-scale mapping of natural  
444 variation in fly fecundity identifies neuronal domain of expression and function of an aquaporin. *PLoS*  
445 *genetics*, 8(4), e1002631. <https://doi.org/10.1371/journal.pgen.1002631>

446 Bischof, J., Maeda, R. K., Hediger, M., Karch, F., & Basler, K. (2007). An optimized  
447 transgenesis system for *Drosophila* using germ-line-specific phiC31 integrases. *Proceedings of the*  
448 *National Academy of Sciences of the United States of America*, 104(9), 3312–3317.  
449 <https://doi.org/10.1073/pnas.0611511104>

450 Choi, J. C., Park, D., & Griffith, L. C. (2004). Electrophysiological and morphological  
451 characterization of identified motor neurons in the *Drosophila* third instar larva central nervous  
452 system. *Journal of neurophysiology*, 91(5), 2353–2365. <https://doi.org/10.1152/jn.01115.2003>

453 Crossley A C. (1978). The morphology and development of the *Drosophila* muscular system.  
454 In: Ashburner M, Wright T, editors. *The genetics and biology of Drosophila*, Vol 2b. Academic; New  
455 York. pp. 499–560.

456 Dhawan, S., Myers, P., Bailey, D., Ostrovsky, A. D., Evers, J. F., & Landgraf, M. (2021).  
457 Reactive Oxygen Species Mediate Activity-Regulated Dendritic Plasticity Through NADPH Oxidase  
458 and Aquaporin Regulation. *Frontiers in cellular neuroscience*, 15, 641802.  
459 <https://doi.org/10.3389/fncel.2021.641802>

460 Dutta, A., & Das, M. (2022). Deciphering the role of aquaporins in metabolic diseases: A mini  
461 review. *The American journal of the medical sciences*, 364(2), 148–162.  
462 <https://doi.org/10.1016/j.amjms.2021.10.029>

463 Fogarty, C. E., Diwanji, N., Lindblad, J. L., Tare, M., Amcheslavsky, A., Makhijani, K.,  
464 Brückner, K., Fan, Y., & Bergmann, A. (2016). Extracellular Reactive Oxygen Species Drive  
465 Apoptosis-Induced Proliferation via *Drosophila* Macrophages. *Current biology: CB*, 26(5), 575–584.  
466 <https://doi.org/10.1016/j.cub.2015.12.064>

467 Frank, C. A., Wang, X., Collins, C. A., Rodal, A. A., Yuan, Q., Verstreken, P., & Dickman, D.  
468 K. (2013). New approaches for studying synaptic development, function, and plasticity using  
469 *Drosophila* as a model system. *The Journal of neuroscience: the official journal of the Society for*  
470 *Neuroscience*, 33(45), 17560–17568. <https://doi.org/10.1523/JNEUROSCI.3261-13.2013>

471 Frank, C. A., Wang, X., Collins, C. A., Rodal, A. A., Yuan, Q., Verstreken, P., & Dickman, D.  
472 K. (2013). New approaches for studying synaptic development, function, and plasticity using

473 Drosophila as a model system. *The Journal of neuroscience: the official journal of the Society for*  
474 *Neuroscience*, 33(45), 17560–17568. <https://doi.org/10.1523/JNEUROSCI.3261-13.2013>

475 Fujioka, M., Lear, B. C., Landgraf, M., Yusibova, G. L., Zhou, J., Riley, K. M., Patel, N. H., &  
476 Jaynes, J. B. (2003). Even-skipped, acting as a repressor, regulates axonal projections in  
477 Drosophila. *Development* (Cambridge, England), 130(22), 5385–5400.  
478 <https://doi.org/10.1242/dev.00770>

479 Goldsmit, Y., Erlich, S., & Pinkas-Kramarski, R. (2001). Neuregulin induces sustained reactive  
480 oxygen species generation to mediate neuronal differentiation. *Cellular and molecular*  
481 *neurobiology*, 21(6), 753–769. <https://doi.org/10.1023/a:1015108306171>

482 Ha, E. M., Lee, K. A., Park, S. H., Kim, S. H., Nam, H. J., Lee, H. Y., Kang, D., & Lee, W. J.  
483 (2009). Regulation of DUOX by the G alpha q-phospholipase C $\beta$ -Ca $^{2+}$  pathway in Drosophila gut  
484 immunity. *Developmental cell*, 16(3), 386–397. <https://doi.org/10.1016/j.devcel.2008.12.015>

485 Ha, E. M., Oh, C. T., Bae, Y. S., & Lee, W. J. (2005). A direct role for dual oxidase in  
486 Drosophila gut immunity. *Science* (New York, N.Y.), 310(5749), 847–850.  
487 <https://doi.org/10.1126/science.1117311>

488 Ha, E. M., Oh, C. T., Ryu, J. H., Bae, Y. S., Kang, S. W., Jang, I. H., Brey, P. T., & Lee, W. J.  
489 (2005b). An antioxidant system required for host protection against gut infection in  
490 Drosophila. *Developmental cell*, 8(1), 125–132. <https://doi.org/10.1016/j.devcel.2004.11.007>

491 Hamada, F. N., Rosenzweig, M., Kang, K., Pulver, S. R., Ghezzi, A., Jegla, T. J., & Garrity, P.  
492 A. (2008). An internal thermal sensor controlling temperature preference in  
493 Drosophila. *Nature*, 454(7201), 217–220. <https://doi.org/10.1038/nature07001>

494 He, T., Nitabach, M. N., & Lnenicka, G. A. (2018). Parvalbumin expression affects synaptic  
495 development and physiology at the Drosophila larval NMJ. *Journal of neurogenetics*, 32(3), 209–220.  
496 <https://doi.org/10.1080/01677063.2018.1498496>

497 Hoang, B., & Chiba, A. (2001). Single-cell analysis of Drosophila larval neuromuscular  
498 synapses. *Developmental biology*, 229(1), 55–70. <https://doi.org/10.1006/dbio.2000.9983>

499 Hongpaisan, J., Winters, C. A., & Andrews, S. B. (2003). Calcium-dependent mitochondrial  
500 superoxide modulates nuclear CREB phosphorylation in hippocampal neurons. *Molecular and cellular*  
501 *neurosciences*, 24(4), 1103–1115. <https://doi.org/10.1016/j.mcn.2003.09.003>

502 Hongpaisan, J., Winters, C. A., & Andrews, S. B. (2004). Strong calcium entry activates  
503 mitochondrial superoxide generation, upregulating kinase signaling in hippocampal neurons. *The*  
504 *Journal of neuroscience : the official journal of the Society for Neuroscience*, 24(48), 10878–10887.  
505 <https://doi.org/10.1523/JNEUROSCI.3278-04.2004>

506 Hussain, A., Pooryasin, A., Zhang, M., Loschek, L. F., La Fortezza, M., Friedrich, A. B., Blais,  
507 C. M., Üçpunar, H. K., Yépez, V. A., Lehmann, M., Gompel, N., Gagneur, J., Sigrist, S. J., & Grunwald  
508 Kadow, I. C. (2018). Inhibition of oxidative stress in cholinergic projection neurons fully rescues  
509 aging-associated olfactory circuit degeneration in *Drosophila*. *eLife*, 7, e32018.  
510 <https://doi.org/10.7554/eLife.32018>

511 Jordán-Álvarez, S., Fouquet, W., Sigrist, S. J., & Acebes, A. (2012). Presynaptic PI3K activity  
512 triggers the formation of glutamate receptors at neuromuscular terminals of *Drosophila*. *Journal of cell  
513 science*, 125(Pt 15), 3621–3629. <https://doi.org/10.1242/jcs.102806>

514 Kamata, H., Oka, S., Shibukawa, Y., Kakuta, J., & Hirata, H. (2005). Redox regulation of nerve  
515 growth factor-induced neuronal differentiation of PC12 cells through modulation of the nerve growth  
516 factor receptor, TrkA. *Archives of biochemistry and biophysics*, 434(1), 16–25.  
517 <https://doi.org/10.1016/j.abb.2004.07.036>

518 Kawahara, T., Quinn, M. T., & Lambeth, J. D. (2007). Molecular evolution of the reactive  
519 oxygen-generating NADPH oxidase (Nox/Duox) family of enzymes. *BMC evolutionary biology*, 7,  
520 109. <https://doi.org/10.1186/1471-2148-7-109>

521 Kempf, A., Song, S. M., Talbot, C. B., & Miesenböck, G. (2019). A potassium channel  $\beta$ -  
522 subunit couples mitochondrial electron transport to sleep. *Nature*, 568(7751), 230–234.  
523 <https://doi.org/10.1038/s41586-019-1034-5>

524 Kishida, K. T., & Klann, E. (2007). Sources and targets of reactive oxygen species in synaptic  
525 plasticity and memory. *Antioxidants & redox signaling*, 9(2), 233–244.  
526 <https://doi.org/10.1089/ars.2007.9.ft-8>

527 Kishida, K. T., Hoeffer, C. A., Hu, D., Pao, M., Holland, S. M., & Klann, E. (2006). Synaptic  
528 plasticity deficits and mild memory impairments in mouse models of chronic granulomatous  
529 disease. *Molecular and cellular biology*, 26(15), 5908–5920. <https://doi.org/10.1128/MCB.00269-06>

530 Knapp, L. T., & Klann, E. (2002). Role of reactive oxygen species in hippocampal long-term  
531 potentiation: contributory or inhibitory?. *Journal of neuroscience research*, 70(1), 1–7.  
532 <https://doi.org/10.1002/jnr.10371>

533 Lachaise, D., Cariou, M. L., David, J. R., Lemeunier, F., Tsacas, L., & Ashburner, M. (1988).  
534 Historical biogeography of the *Drosophila melanogaster* species subgroup. In *Evolutionary  
535 biology* (pp. 159-225). Springer, Boston, MA

536 Lam, A. J., St-Pierre, F., Gong, Y., Marshall, J. D., Cranfill, P. J., Baird, M. A., McKeown, M.  
537 R., Wiedenmann, J., Davidson, M. W., Schnitzer, M. J., Tsien, R. Y., & Lin, M. Z. (2012). Improving

538 FRET dynamic range with bright green and red fluorescent proteins. *Nature methods*, 9(10), 1005–  
539 1012. <https://doi.org/10.1038/nmeth.2171>

540 Lambeth J. D. (2002). Nox/Duox family of nicotinamide adenine dinucleotide (phosphate)  
541 oxidases. *Current opinion in hematology*, 9(1), 11–17. <https://doi.org/10.1097/00062752-200201000-00003>

542 Landgraf, M., Bossing, T., Technau, G. M., & Bate, M. (1997). The origin, location, and  
543 projections of the embryonic abdominal motorneurons of *Drosophila*. *The Journal of neuroscience: the  
544 official journal of the Society for Neuroscience*, 17(24), 9642–9655.  
545 <https://doi.org/10.1523/JNEUROSCI.17-24-09642.1997>

546 Landgraf, M., Jeffrey, V., Fujioka, M., Jaynes, J. B., & Bate, M. (2003). Embryonic origins of  
547 a motor system: motor dendrites form a myotopic map in *Drosophila*. *PLoS biology*, 1(2), E41.  
548 <https://doi.org/10.1371/journal.pbio.0000041>

549 Martín-Peña, A., Acebes, A., Rodríguez, J. R., Sorribes, A., de Polavieja, G. G., Fernández-  
550 Fúnez, P., & Ferrús, A. (2006). Age-independent synaptogenesis by phosphoinositide 3 kinase. *The  
551 Journal of neuroscience: the official journal of the Society for Neuroscience*, 26(40), 10199–10208.  
552 <https://doi.org/10.1523/JNEUROSCI.1223-06.2006>

553 Martins, R. N., Harper, C. G., Stokes, G. B., & Masters, C. L. (1986). Increased cerebral  
554 glucose-6-phosphate dehydrogenase activity in Alzheimer's disease may reflect oxidative  
555 stress. *Journal of neurochemistry*, 46(4), 1042–1045. <https://doi.org/10.1111/j.1471-4159.1986.tb00615.x>

556 Massaad, C. A., & Klann, E. (2011). Reactive oxygen species in the regulation of synaptic  
557 plasticity and memory. *Antioxidants & redox signaling*, 14(10), 2013–2054.  
558 <https://doi.org/10.1089/ars.2010.3208>

559 Millana Fañanás, E., Todesca, S., Sicorello, A., Masino, L., Pompach, P., Magnani, F., Pastore,  
560 A., & Mattevi, A. (2020). On the mechanism of calcium-dependent activation of NADPH oxidase 5  
561 (NOX5). *The FEBS journal*, 287(12), 2486–2503. <https://doi.org/10.1111/febs.15160>

562 Millana Fañanás, E., Todesca, S., Sicorello, A., Masino, L., Pompach, P., Magnani, F., Pastore,  
563 A., & Mattevi, A. (2020). On the mechanism of calcium-dependent activation of NADPH oxidase 5  
564 (NOX5). *The FEBS journal*, 287(12), 2486–2503. <https://doi.org/10.1111/febs.15160>

565 Milton, V. J., Jarrett, H. E., Gowers, K., Chalak, S., Briggs, L., Robinson, I. M., & Sweeney,  
566 S. T. (2011). Oxidative stress induces overgrowth of the *Drosophila* neuromuscular  
567 junction. *Proceedings of the National Academy of Sciences of the United States of America*, 108(42),  
568 17521–17526. <https://doi.org/10.1073/pnas.1014511108>

571 Moreira, S., Stramer, B., Evans, I., Wood, W., & Martin, P. (2010). Prioritization of competing  
572 damage and developmental signals by migrating macrophages in the *Drosophila* embryo. *Current  
573 biology: CB*, 20(5), 464–470. <https://doi.org/10.1016/j.cub.2010.01.047>

574 Munnamalai, V., & Suter, D. M. (2009). Reactive oxygen species regulate F-actin dynamics in  
575 neuronal growth cones and neurite outgrowth. *Journal of neurochemistry*, 108(3), 644–661.  
576 <https://doi.org/10.1111/j.1471-4159.2008.05787.x>

577 Munnamalai, V., Weaver, C. J., Weisheit, C. E., Venkatraman, P., Agim, Z. S., Quinn, M. T.,  
578 & Suter, D. M. (2014). Bidirectional interactions between NOX2-type NADPH oxidase and the F-actin  
579 cytoskeleton in neuronal growth cones. *Journal of neurochemistry*, 130(4), 526–540.  
580 <https://doi.org/10.1111/jnc.12734>

581 Murphy M. P. (2009). How mitochondria produce reactive oxygen species. *The Biochemical  
582 journal*, 417(1), 1–13. <https://doi.org/10.1042/BJ20081386>

583 Niethammer P. (2016). The early wound signals. *Current opinion in genetics &  
584 development*, 40, 17–22. <https://doi.org/10.1016/j.gde.2016.05.001>

585 Niethammer, P., Grabher, C., Look, A. T., & Mitchison, T. J. (2009). A tissue-scale gradient  
586 of hydrogen peroxide mediates rapid wound detection in zebrafish. *Nature*, 459(7249), 996–999.  
587 <https://doi.org/10.1038/nature08119>

588 Nitti, M., Furfaro, A. L., Cevasco, C., Traverso, N., Marinari, U. M., Pronzato, M. A., &  
589 Domenicotti, C. (2010). PKC delta and NADPH oxidase in retinoic acid-induced neuroblastoma cell  
590 differentiation. *Cellular signalling*, 22(5), 828–835. <https://doi.org/10.1016/j.cellsig.2010.01.007>

591 Olguín-Albuerne, M., & Morán, J. (2015). ROS produced by NOX2 control in vitro  
592 development of cerebellar granule neurons development. *ASN neuro*, 7(2), 1759091415578712.  
593 <https://doi.org/10.1177/1759091415578712>

594 Oswald, M. C., Brooks, P. S., Zwart, M. F., Mukherjee, A., West, R. J., Giachello, C. N.,  
595 Morarach, K., Baines, R. A., Sweeney, S. T., & Landgraf, M. (2018a). Reactive oxygen species  
596 regulate activity-dependent neuronal plasticity in *Drosophila*. *eLife*, 7, e39393.  
597 <https://doi.org/10.7554/eLife.39393>

598 Oswald, M., Garnham, N., Sweeney, S. T., & Landgraf, M. (2018b). Regulation of neuronal  
599 development and function by ROS. *FEBS letters*, 592(5), 679–691. [https://doi.org/10.1002/1873-3468.12972](https://doi.org/10.1002/1873-<br/>600 3468.12972)

601 Ou, Y., Chwalla, B., Landgraf, M., & van Meyel, D. J. (2008). Identification of genes  
602 influencing dendrite morphogenesis in developing peripheral sensory and central motor  
603 neurons. *Neural development*, 3, 16. <https://doi.org/10.1186/1749-8104-3-16>

604 Owusu-Ansah, E., & Banerjee, U. (2009). Reactive oxygen species prime Drosophila  
605 haematopoietic progenitors for differentiation. *Nature*, 461(7263), 537–541.  
606 <https://doi.org/10.1038/nature08313>

607 Panday, A., Sahoo, M. K., Osorio, D., & Batra, S. (2015). NADPH oxidases: an overview from  
608 structure to innate immunity-associated pathologies. *Cellular & molecular immunology*, 12(1), 5–23.  
609 <https://doi.org/10.1038/cmi.2014.89>

610 Peng, J. J., Lin, S. H., Liu, Y. T., Lin, H. C., Li, T. N., & Yao, C. K. (2019). A circuit-dependent  
611 ROS feedback loop mediates glutamate excitotoxicity to sculpt the Drosophila motor system. *eLife*, 8,  
612 e47372. <https://doi.org/10.7554/eLife.47372>

613 Pérez-Moreno, J. J., & O'Kane, C. J. (2019). GAL4 Drivers Specific for Type Ib and Type Is  
614 Motor Neurons in Drosophila. *G3* (Bethesda, Md.), 9(2), 453–462.  
615 <https://doi.org/10.1534/g3.118.200809>

616 Pool, J. E., Corbett-Detig, R. B., Sugino, R. P., Stevens, K. A., Cardeno, C. M., Crepeau, M.  
617 W., Duchen, P., Emerson, J. J., Saelao, P., Begun, D. J., & Langley, C. H. (2012). Population Genomics  
618 of sub-saharan *Drosophila melanogaster*: African diversity and non-African admixture. *PLoS*  
619 genetics, 8(12), e1003080. <https://doi.org/10.1371/journal.pgen.1003080>

620 Pulver, S. R., Pashkovski, S. L., Hornstein, N. J., Garrity, P. A., & Griffith, L. C. (2009).  
621 Temporal dynamics of neuronal activation by Channelrhodopsin-2 and TRPA1 determine behavioral  
622 output in Drosophila larvae. *Journal of neurophysiology*, 101(6), 3075–3088.  
623 <https://doi.org/10.1152/jn.00071.2009>

624 Razzell, W., Evans, I. R., Martin, P., & Wood, W. (2013). Calcium flashes orchestrate the  
625 wound inflammatory response through DUOX activation and hydrogen peroxide release. *Current*  
626 *biology: CB*, 23(5), 424–429. <https://doi.org/10.1016/j.cub.2013.01.058>

627 Rhee, S. G. (1999). Redox signaling: hydrogen peroxide as intracellular  
628 messenger. *Experimental & molecular medicine*, 31(2), 53–59. <https://doi.org/10.1038/emm.1999.9>

629 Rigutto, S., Hoste, C., Grasberger, H., Milenkovic, M., Communi, D., Dumont, J. E., Corvilain,  
630 B., Miot, F., & De Deken, X. (2009). Activation of dual oxidases Duox1 and Duox2: differential  
631 regulation mediated by camp-dependent protein kinase and protein kinase C-dependent  
632 phosphorylation. *The Journal of biological chemistry*, 284(11), 6725–6734.  
633 <https://doi.org/10.1074/jbc.M806893200>

634 Rigutto, S., Hoste, C., Grasberger, H., Milenkovic, M., Communi, D., Dumont, J. E., Corvilain,  
635 B., Miot, F., & De Deken, X. (2009). Activation of dual oxidases Duox1 and Duox2: differential  
636 regulation mediated by camp-dependent protein kinase and protein kinase C-dependent

637 phosphorylation. *The Journal of biological chemistry*, 284(11), 6725–6734.  
638 <https://doi.org/10.1074/jbc.M806893200>

639 Sanz A. (2016). Mitochondrial reactive oxygen species: Do they extend or shorten animal  
640 lifespan?. *Biochimica et biophysica acta*, 1857(8), 1116–1126.  
641 <https://doi.org/10.1016/j.bbabi.2016.03.018>

642 Sauer, H., Wartenberg, M., & Hescheler, J. (2001). Reactive oxygen species as intracellular  
643 messengers during cell growth and differentiation. *Cellular physiology and biochemistry : international  
644 journal of experimental cellular physiology, biochemistry, and pharmacology*, 11(4), 173–186.  
645 <https://doi.org/10.1159/000047804>

646 Serrano, F., Kolluri, N. S., Wientjes, F. B., Card, J. P., & Klann, E. (2003). NADPH oxidase  
647 immunoreactivity in the mouse brain. *Brain research*, 988(1-2), 193–198.  
648 [https://doi.org/10.1016/s0006-8993\(03\)03364-x](https://doi.org/10.1016/s0006-8993(03)03364-x)

649 Shearin, H. K., Macdonald, I. S., Spector, L. P., & Stowers, R. S. (2014). Hexameric GFP and  
650 mCherry reporters for the *Drosophila* GAL4, Q, and LexA transcription systems. *Genetics*, 196(4),  
651 951–960. <https://doi.org/10.1534/genetics.113.161141>

652 Sink, H., & Whitington, P. M. (1991). Location and connectivity of abdominal motoneurons in  
653 the embryo and larva of *Drosophila melanogaster*. *Journal of neurobiology*, 22(3), 298–311.  
654 <https://doi.org/10.1002/neu.480220309>

655 Spina, M. B., & Cohen, G. (1989). Dopamine turnover and glutathione oxidation: implications  
656 for Parkinson disease. *Proceedings of the National Academy of Sciences of the United States of  
657 America*, 86(4), 1398–1400. <https://doi.org/10.1073/pnas.86.4.1398>

658 Suzukawa, K., Miura, K., Mitsushita, J., Resau, J., Hirose, K., Crystal, R., & Kamata, T. (2000).  
659 Nerve growth factor-induced neuronal differentiation requires generation of Rac1-regulated reactive  
660 oxygen species. *The Journal of biological chemistry*, 275(18), 13175–13178.  
661 <https://doi.org/10.1074/jbc.275.18.13175>

662 Tejada-Simon, M. V., Serrano, F., Villasana, L. E., Kanterewicz, B. I., Wu, G. Y., Quinn, M.  
663 T., & Klann, E. (2005). Synaptic localization of a functional NADPH oxidase in the mouse  
664 hippocampus. *Molecular and cellular neurosciences*, 29(1), 97–106.  
665 <https://doi.org/10.1016/j.mcn.2005.01.007>

666 Terzi, A., & Suter, D. M. (2020). The role of NADPH oxidases in neuronal development. *Free  
667 radical biology & medicine*, 154, 33–47. <https://doi.org/10.1016/j.freeradbiomed.2020.04.027>

668 Tsai, P. I., Wang, M., Kao, H. H., Cheng, Y. J., Lin, Y. J., Chen, R. H., & Chien, C. T. (2012).  
669 Activity-dependent retrograde laminin A signaling regulates synapse growth at *Drosophila*

670 neuromuscular junctions. *Proceedings of the National Academy of Sciences of the United States of*  
671 *America*, 109(43), 17699–17704. <https://doi.org/10.1073/pnas.1206416109>

672 Ushio-Fukai M. (2009). Compartmentalization of redox signaling through NADPH oxidase-  
673 derived ROS. *Antioxidants & redox signaling*, 11(6), 1289–1299. doi:10.1089/ars.2008.2333

674 Wilson, C., & González-Billault, C. (2015). Regulation of cytoskeletal dynamics by redox  
675 signaling and oxidative stress: implications for neuronal development and trafficking. *Frontiers in*  
676 *cellular neuroscience*, 9, 381. <https://doi.org/10.3389/fncel.2015.00381>

677 Wilson, C., Muñoz-Palma, E., & González-Billault, C. (2018). From birth to death: A role for  
678 reactive oxygen species in neuronal development. *Seminars in cell & developmental biology*, 80, 43–  
679 49. <https://doi.org/10.1016/j.semcd.2017.09.012>

680 Wilson, C., Muñoz-Palma, E., Henríquez, D. R., Palmisano, I., Núñez, M. T., Di Giovanni, S.,  
681 & González-Billault, C. (2016). A Feed-Forward Mechanism Involving the NOX Complex and RyR-  
682 Mediated Ca<sup>2+</sup> Release During Axonal Specification. *The Journal of neuroscience: the official journal*  
683 *of the Society for Neuroscience*, 36(43), 11107–11119. <https://doi.org/10.1523/JNEUROSCI.1455-16.2016>

685 Wilson, C., Núñez, M. T., & González-Billault, C. (2015). Contribution of NADPH oxidase to  
686 the establishment of hippocampal neuronal polarity in culture. *Journal of cell science*, 128(16), 2989–  
687 2995. <https://doi.org/10.1242/jcs.168567>

688 Zarin, A. A., Mark, B., Cardona, A., Litwin-Kumar, A., & Doe, C. Q. (2019). A multilayer  
689 circuit architecture for the generation of distinct locomotor behaviors in *Drosophila*. *eLife*, 8, e51781.  
690 <https://doi.org/10.7554/eLife.51781>

691 Zhong, Y., Budnik, V., & Wu, C. F. (1992). Synaptic plasticity in *Drosophila* memory and  
692 hyperexcitable mutants: role of cAMP cascade. *The Journal of neuroscience: the official journal of the*  
693 *Society for Neuroscience*, 12(2), 644–651. <https://doi.org/10.1523/JNEUROSCI.12-02-00644.1992>

694 Zorov, D. B., Juhaszova, M., & Sollott, S. J. (2014). Mitochondrial reactive oxygen species  
695 (ROS) and ROS-induced ROS release. *Physiological reviews*, 94(3), 909–950.  
696 <https://doi.org/10.1152/physrev.00026.2013>

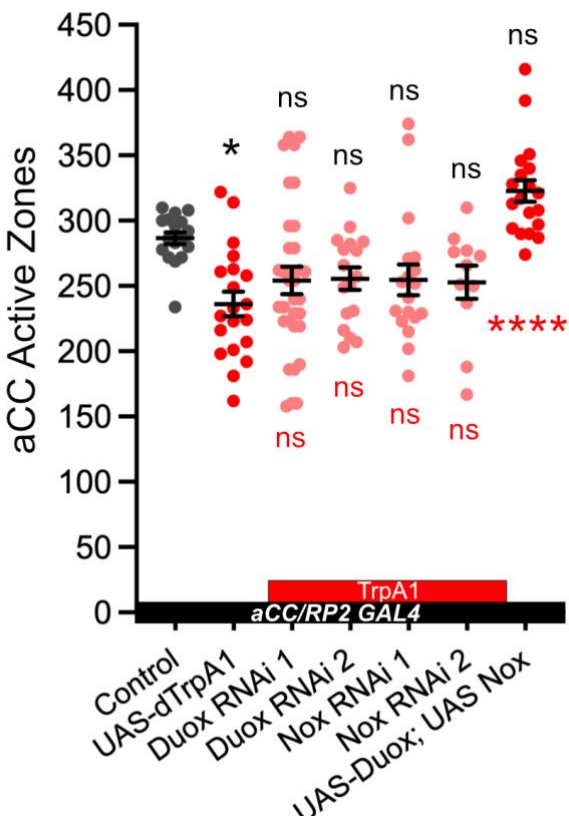
697 Zucker, R. S., & Regehr, W. G. (2002). Short-term synaptic plasticity. *Annual review of*  
698 *physiology*, 64, 355–405. <https://doi.org/10.1146/annurev.physiol.64.092501.114547>

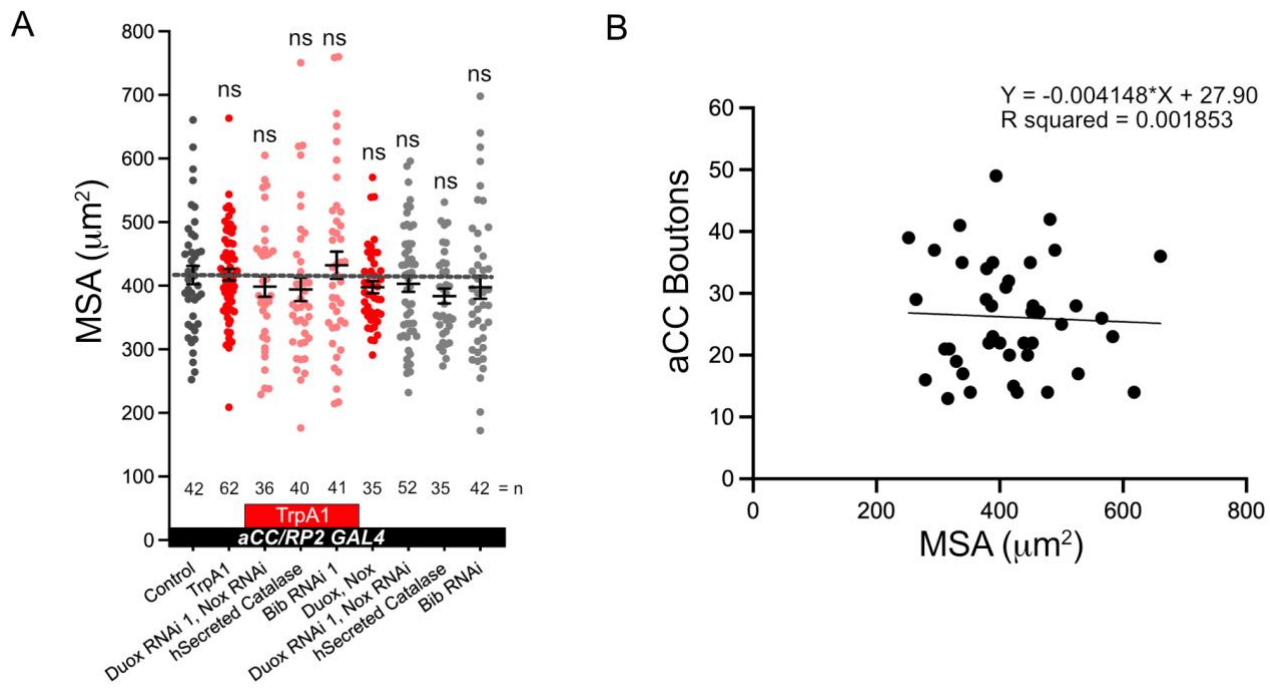
699

700

701

702 6 Supplementary Figures





709

710 **Supplementary Figure 2. Muscles size.** A) Dot-plot quantification shows no statistically  
711 significant differences between genotypes in average muscle surface area (MSA). Mean  $\pm$  SEM,  
712 Kruskal-Wallis test. B) Linear regression using the control data shows not correlation between  
713 aCC NMJ terminal bouton numbers and muscle size,  $p$ -value = 0.7866.

714

715

716

## 717 7 Author Contributions

718 D.S.C, M.C.W.O, A.M. and M.L. conceived of the study and wrote the manuscript. D.M.D.B. cloned  
719 Duox and Nox transgenes. M.L. generated transgenic stocks. D.S.C. and M.C.W.O. carried out all  
720 experiments and analysed data.

721 8 Funding

722 This work was made possible through support by the Biotechnology and Biological Sciences  
723 Research Council (BBSRC) to M.L. (BB/R016666/1 and BB/V014943/1). D.S.-C. was supported by  
724 the European Molecular Biology Organization (EMBO) with a long-term EMBO fellowship (ALTF  
725 62-2021) and a John Stanley Gardiner studentship to A.M. The work benefited from the Imaging

726 Facility, Department of Zoology, supported by Matt Wayland and funds from a Wellcome Trust  
727 Equipment Grant (WT079204) with contributions by the Sir Isaac Newton Trust in Cambridge,  
728 including Research Grant [18.07ii(c)].

729 **9 Acknowledgments**

730 The authors would like to thank Niklas Krick for feedback on the manuscript. The authors are  
731 grateful to Andreas Bergmann, Paul Garrity, Won-Jae Lee, Paul Martin, Sean Sweeney, Helen  
732 Weavers, and Will Wood, as well as the Bloomington Drosophila Stock Center and Vienna  
733 Drosophila Resource Centre for generously providing fly stocks; and to Won-Jae Lee for providing  
734 DNA containing Duox cDNA, and the Drosophila Genomics Resource Center (DGRC), supported by  
735 NIH grant 2P40OD010949, for clone FI15205 containing Nox cDNA.